
Aligning Time Series on Incomparable Spaces

Samuel Cohen
University College London

Giulia Luise
University College London

Alexander Terenin
Imperial College London

Brandon Amos
Facebook AI Research

Marc Peter Deisenroth
University College London

Abstract

Dynamic time warping (DTW) is a useful method for aligning, comparing and combining time series, but it requires them to live in comparable spaces. In this work, we consider a setting in which time series live on different spaces without a sensible ground metric, causing DTW to become ill-defined. To alleviate this, we propose Gromov dynamic time warping (GDTW), a distance between time series on potentially incomparable spaces that avoids the comparability requirement by instead considering intra-relational geometry. We derive a Frank–Wolfe algorithm for computing it and demonstrate its effectiveness at aligning, combining and comparing time series living on incomparable spaces. We further propose a smoothed version of GDTW as a differentiable loss and assess its properties in a variety of settings, including barycentric averaging, generative modeling and imitation learning.

1 Introduction

Data is often gathered sequentially in the form of a time series, which consists of sequences of data points observed at successive time points. Elements of such sequences are correlated through time, and comparing time series requires one to take the direction of time into account. To define a sensible similarity measure between time series, Sakoe and Chiba [21] proposed *dynamic time warping* (DTW), a distance over the space of time series, which has recently been extended by Cuturi and Blondel [6] into soft DTW for use as a differentiable loss. DTW consists of a minimal-cost alignment problem and is solved via a Bellman recursion, while soft DTW leverages a soft-min operation to smooth the DTW objective. Such distances enable tackling a large range of temporal problems, including aligning time series, averaging them or making long-term predictions.

DTW-based approaches require a sensible cost function between samples from the two time series. The specification of such cost functions is often hard, and limits the applicability of DTW. For example, in cases where the time series are invariant under symmetries, such as sequences of word embeddings which are only identified up to a rotation of latent space, one needs to solve an alignment problem to compare the two sequences. Vayer et al. [25] propose an extension of DTW that addresses this issue by making the cost invariant with respect to specific sets of symmetries. In this case, one still requires the definition of a cost function between samples from the two time series, along with a potentially large set of transformations to optimize over. On the other hand, in multi-modal settings, one considers time series that live on incomparable spaces: for example, the configuration space of a physical system and its representation as pixels of a video frame. In such cases, defining a sensible distance between samples from the two sequences is impractical, as it would require detailed understanding of the objects we wish to study.

In this work, we propose to tackle the problem by relaxing our notion of equality in a manner inspired by recent ideas from the optimal transport literature. Using connections between DTW and the

Preprint. Under review.

Code available at: [HTTPS://GITHUB.COM/SAMCOHEN16/ALIGNING-TIME-SERIES](https://github.com/samcohen16/aligning-time-series)

Wasserstein distance, we propose *Gromov dynamic time warping* (GDTW), which compares two time series by contrasting their intra-relational geometries, analogously to the Gromov-Wasserstein distance of isometry classes of metric-measure spaces [16]. This allows one to compare two time series without defining a sensible ground cost between their domains, and automatically incorporates invariances into the distance.

Contributions. (1) We introduce Gromov DTW, a distance between time series and a smoothed version extending DTW variants to handling time series on incomparable space, (2) we present an efficient algorithm for computing it, (3) we apply Gromov DTW to a range of settings including barycentric averaging, generative modeling and imitation learning.

Notation. Let $(\mathcal{X}, d_{\mathcal{X}})$ be a compact metric space, and let a *time series* \mathbf{x} of length $T \in \mathbb{N}$ be an element of \mathcal{X}^T . Let $\mathcal{A}(m, n) \subseteq \{0, 1\}^{m \times n}$ be the set of *alignment matrices*, which are binary matrices containing a path of ones from the top-left to the bottom-right corner, allowing only bottom, right or diagonal bottom-right moves. Given a matrix $\mathbf{A} \in \mathcal{A}(m, n)$ and a 4-dimensional array $\mathbf{L} \in \mathbb{R}^{m \times n \times m \times n}$, define the matrix $(\mathbf{L} \otimes \mathbf{A})_{ij} = (\sum_{kl} L_{ijkl} A_{kl})_{ij}$. Denote the Frobenius matrix inner product by $\langle \cdot, \cdot \rangle_{\text{F}}$. Define the probability simplex $\Delta_J := \{q \in \mathbb{R}^J, q_j \geq 0 \text{ for } j = 1, \dots, J, \sum_j q_j = 1\}$. Finally, $\mathbf{x}_{:i}$ corresponds to the first i time steps of \mathbf{x} .

2 Background and Related Work

We now introduce concepts and definitions needed in the rest of the work.

2.1 Dynamic Time Warping for Time Series Alignment

We now review DTW and its smoothed version. Sakoe and Chiba [21] consider the problem of aligning two time series $\mathbf{x} \in \mathcal{X}^{T_x}$ and $\mathbf{y} \in \mathcal{X}^{T_y}$, where potentially $T_x \neq T_y$. This is formalized as

$$\text{DTW}(\mathbf{x}, \mathbf{y}) = \min_{\mathbf{A} \in \mathcal{A}(T_x, T_y)} \langle \mathbf{D}, \mathbf{A} \rangle_{\text{F}}, \quad (1)$$

where $D_{ij} = d_{\mathcal{X}}(x_i, y_j)$ is the pairwise distance matrix. This problem amounts to finding an alignment matrix that minimizes the total alignment cost. The objective (1) can be computed in $O(T_x T_y)$ by leveraging the dynamic programming forward recursion

$$\text{DTW}(\mathbf{x}_{:i}, \mathbf{y}_{:j}) = d_{\mathcal{X}}(\mathbf{x}_i, \mathbf{y}_j) + \min(\text{DTW}(\mathbf{x}_{:i-1}, \mathbf{y}_{:j-1}), \text{DTW}(\mathbf{x}_{:i-1}, \mathbf{y}_{:j}), \text{DTW}(\mathbf{x}_{:i}, \mathbf{y}_{:j-1})). \quad (2)$$

The optimal alignment matrix \mathbf{A}^* can then be obtained by tracking the optimal path backwards. DTW is a more flexible choice for comparing time series than element-wise Euclidean distances, because it allows one to compare time series of different sampling frequencies due to its ability to warp time. In particular, two time series can be close in DTW even if $T_x \neq T_y$. DTW has been used in a number of settings, including time series averaging and clustering [18, 22] and feature extraction [2, 12].

A limitation of DTW is the discontinuity of its gradient, which can affect the performance of gradient descent algorithms. To address this, Cuturi and Blondel [6] introduced a soft version of DTW. The minimum in (1) is replaced with a softened version, yielding

$$\text{DTW}_{\gamma}(\mathbf{x}, \mathbf{y}) = -\gamma \log \sum_{\mathbf{A} \in \mathcal{A}(T_x, T_y)} \exp\left(-\frac{1}{\gamma} \langle \mathbf{D}, \mathbf{A} \rangle_{\text{F}}\right). \quad (3)$$

DTW is recovered in the limit $\gamma \rightarrow 0$. They also discuss a softened version of the optimal alignment matrix \mathbf{A}^* , given by the softened argmin defined by

$$\arg \min_{\mathbf{A} \in \mathcal{A}(m, n)}^{\gamma} \langle \mathbf{D}, \mathbf{A} \rangle_{\text{F}} = \frac{1}{C_{\mathbf{x}, \mathbf{y}}} \sum_{\mathbf{A} \in \mathcal{A}(T_x, T_y)} \exp\left(-\frac{1}{\gamma} \langle \mathbf{D}, \mathbf{A} \rangle_{\text{F}}\right) \mathbf{A}, \quad (4)$$

where $C_{\mathbf{x}, \mathbf{y}}$ is the normalizing constant of the unnormalized density $e^{-\frac{1}{\gamma} \langle \mathbf{D}, \mathbf{A} \rangle_{\text{F}}}$. While it considers temporal variability, DTW is not invariant under transformations, such as translations and rotations, which can limit its application to settings where time series are obtained only up to isometric transformations, such as word embeddings. To alleviate this, Vayer et al. [25] propose

$$\text{DTW-GI}(\mathbf{x}, \mathbf{y}) = \min_{f \in \mathcal{F}} \text{DTW}(\mathbf{x}, f(\mathbf{y})) \quad (5)$$

which gives a distance between time series that is invariant under a set of transformations \mathcal{F} where f is applied elementwise to points of the time series, and Vayer et al. [25] consider orthonormal transformations. However, in more general settings, this requires one to optimize over a potentially large space of transformations \mathcal{F} , which becomes unfeasible if \mathbf{x} and \mathbf{y} are too different.

2.2 Connecting DTW and Optimal Transport

Optimal transport [19] allows one to compare and average measures in a way that incorporates the geometry of the underlying space on which they are defined. Such approaches can be intuitively connected to DTW by observing that time series are essentially discrete measures equipped with an ordering. This allows one to view the alignment matrices in the DTW objective as analogues of coupling matrices that appear in the Kantorovich formulation of the classical optimal transport problem [27]. To formalize this, we introduce the Wasserstein distance between discrete measures. Let $\mu_x = \sum_{i=1}^m p_i \delta_{x_i}$, $\mu_y = \sum_{i=1}^n q_i \delta_{y_i}$ be discrete probability measures with $\mathbf{p} \in \Delta_m$, $\mathbf{q} \in \Delta_n$, and set $D_{ij} = d_{\mathcal{X}}(x_i, x_j)$. Define the Wasserstein distance between discrete measures μ_x and μ_y as

$$W(\mu_x, \mu_y) = \min_{\mathbf{T} \in \Pi(\mathbf{p}, \mathbf{q})} \langle \mathbf{D}, \mathbf{T} \rangle_{\mathbb{F}} \quad (6)$$

where $\Pi(\mathbf{p}, \mathbf{q})$ is the set of coupling matrices with marginals \mathbf{p} and \mathbf{q} . Equation (6) clearly resembles (1), and in both cases the objective consists of the minimization of the element-wise dot product between a distance matrix and another matrix, which we call the *plan*. In the DTW case, the plan consists of an alignment matrix, and in the Wasserstein case it consists of a coupling matrix. Moreover, the optimal coupling T_{ij}^* describes the optimal amount of probability mass to move from point x_i to y_j , whilst the optimal alignment A_{ij}^* describes whether or not x_i and y_j are aligned at optimality.

The Wasserstein distance is limited by the requirement for a sensible ground metric to be defined between samples $x_i \in \mathcal{X}$ and $y_j \in \mathcal{Y}$, which is impossible if the spaces are unregistered [24]. The Wasserstein distance is also not invariant under isometries, such as rotations and translations, and generally leads to a large distance between measures equivalent up to such transformations. To relax these requirements, Mémoli [16] proposed the Gromov–Wasserstein (GW) distance between metric-measure triples $(\mathcal{X}, d_{\mathcal{X}}, \mu_x)$ and $(\mathcal{Y}, d_{\mathcal{Y}}, \mu_y)$, up to isometry. It is defined as

$$\text{GW}(\mu_x, \mu_y) = \min_{\mathbf{T} \in \Pi(\mathbf{p}, \mathbf{q})} \sum_{ijkl} \mathcal{L}(d_{\mathcal{X}}(x_i, x_k), d_{\mathcal{Y}}(y_j, y_l)) T_{ij} T_{kl} \quad (7)$$

where \mathcal{L} is typically squared error loss or Kullback-Leibler divergence, and does not rely on a cost or metric to compare x_i with y_j . GW compares the intra-relational metric geometries of the two measures by comparing the distributions of their pairwise distances, and only requires the definition of metrics $d_{\mathcal{X}}$ and $d_{\mathcal{Y}}$ on \mathcal{X} and \mathcal{Y} , respectively, which can be arbitrarily different. GW has been used as a tool for comparing measures on incomparable spaces, notably for training generative models [1], graph matching [29], and graph averaging [28]. Vayer et al. [26] also proposed an extension of both Wasserstein and GW, named Fused-Gromov-Wasserstein to deal with structured measures such as graphs, which consists of a mixture of Wasserstein distances on the structural components, and GW on the spatial features.

3 Gromov Dynamic Time Warping

Motivated by the connections between DTW and optimal transport described in Sections 2.1 and 2.2, respectively, we introduce a distance between time series $\mathbf{x} \in \mathcal{X}^{T_x}$ and $\mathbf{y} \in \mathcal{Y}^{T_y}$ defined on potentially incomparable compact metric spaces. Define the *Gromov dynamic time warping* distance between metric-time-series triples $(\mathcal{X}, d_{\mathcal{X}}, \mathbf{x})$ and $(\mathcal{Y}, d_{\mathcal{Y}}, \mathbf{y})$ as

$$\text{GDTW}(\mathbf{x}, \mathbf{y}) = \min_{\mathbf{A} \in \mathcal{A}(T_x, T_y)} \sum_{ijkl} \mathcal{L}(d_{\mathcal{X}}(x_i, x_k), d_{\mathcal{Y}}(y_j, y_l)) A_{ij} A_{kl} \quad (8)$$

where $\mathcal{L} : \mathbb{R}^2 \rightarrow \mathbb{R}^+$ is a loss function measuring the alignment of the pairwise distances, and the first two elements of the triple are omitted to ease notation. We think of \mathcal{L} as a proxy for measuring the alignment of the time series (e.g. the square error loss $\mathcal{L}(a, b) = (a - b)^2$ and KL loss $\mathcal{L}(a, b) = \text{KL}(a || b) = a \log(\frac{a}{b}) - a + b$). Under the optimal alignment, for any two pairs (x_i, y_j) and (x_k, y_l) , if x_i is close to x_k then y_j is close to y_l . Some optimal alignments are given in Figure 1.

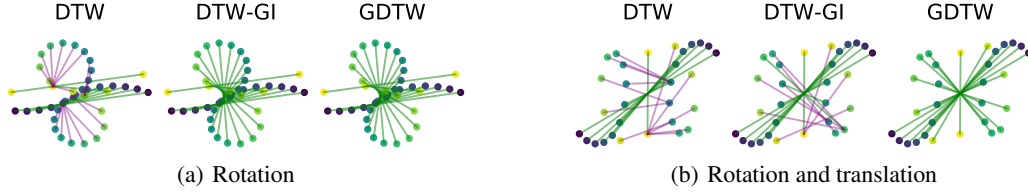


Figure 1: Alignment of time series equivalent (a) up to rotation by 180 degrees, and (b) equivalent up to rotation and translation (respectively green and purple for correct and incorrect matchings).

Provided \mathcal{L} is a pre-metric and so induces a Hausdorff topology, GDTW possesses the following properties: (i) $\text{GDTW}(\mathbf{x}, \mathbf{y}) \geq 0$, and $\text{GDTW}(\mathbf{x}, \mathbf{x}) = 0$, (ii) $\text{GDTW}(\mathbf{x}, \mathbf{y}) = 0$ if and only if there exists an isometry $\phi: \mathcal{X} \rightarrow \mathcal{Y}$ such that $\phi(\mathbf{x}) = \mathbf{y}$, and (iii) $\text{GDTW}(\mathbf{y}, \mathbf{x}) = \text{GDTW}(\mathbf{x}, \mathbf{y})$ if and only if \mathcal{L} is symmetric. As DTW fails to satisfy the triangle inequality, GDTW does not generally satisfy it either. Thus, GDTW is a pre-metric over equivalence classes of $(\mathcal{X}, d_{\mathcal{X}}, \mathbf{x})$, up to metric isometry. A formal treatment is given in Appendix A.

3.1 Efficient Computation via a Frank–Wolfe Algorithm

We now present a straightforward algorithm for computing GDTW. Following ideas proposed in the optimal transport setting for computing the Gromov–Wasserstein distance, one can introduce a 4-dimensional array $L_{ijkl} = \mathcal{L}(d_{\mathcal{X}}(x_i, x_k), d_{\mathcal{Y}}(y_j, y_l))$ and express GDTW as

$$\text{GDTW}(\mathbf{x}, \mathbf{y}) = \min_{\mathbf{A} \in \mathcal{A}(T_x, T_y)} \mathcal{G}_{\mathbf{x}, \mathbf{y}}(\mathbf{A}), \quad \mathcal{G}_{\mathbf{x}, \mathbf{y}}(\mathbf{A}) = \langle \mathbf{L} \otimes \mathbf{A}, \mathbf{A} \rangle_{\text{F}}. \quad (9)$$

This expression is similar to the DTW objective in (1), but with a cost function \mathbf{D} that now depends on the alignment matrix \mathbf{A} . We apply the Frank–Wolfe algorithm [4, 9] to (9). This consists of (i) solving a linear minimization oracle

$$\mathbf{S}^{(t)} = \arg \min_{\mathbf{A} \in \mathcal{A}(T_x, T_y)} \langle \nabla_{\mathbf{A}} \mathcal{G}_{\mathbf{x}, \mathbf{y}}(\mathbf{A}^{(t)}), \mathbf{A} \rangle = \arg \min_{\mathbf{A} \in \mathcal{A}(T_x, T_y)} \langle \mathbf{L} \otimes \mathbf{A}^{(t)}, \mathbf{A} \rangle, \quad (10)$$

which can be performed exactly in $O(T_x T_y)$ by a DTW iteration, and we note that $\mathbf{L} \otimes \mathbf{A}^{(t)}$ can be computed in $O(T_x^2 T_y + T_x T_y^2)$ in the case $\mathcal{L} = L_2$ [20]. This is followed by (ii) a line-search step

$$\eta^{(t)} = \arg \min_{\eta \in [0, 1]} \mathcal{G}_{\mathbf{x}, \mathbf{y}}(\mathbf{A}^{(t)} + \eta(\mathbf{S}^{(t)} - \mathbf{A}^{(t)})) \in \{0, 1\}. \quad (11)$$

We prove in Appendix A that the optimal step size is always 0 or 1. The final step (iii) is updating

$$\mathbf{A}^{(t+1)} = \mathbf{A}^{(t)} + \eta^{(t)}(\mathbf{S}^{(t)} - \mathbf{A}^{(t)}) = \begin{cases} \mathbf{A}^{(t)} & \text{if } \eta^{(t)} = 0, \\ \mathbf{S}^{(t)} & \text{if } \eta^{(t)} = 1. \end{cases} \quad (12)$$

In summary: if $\mathbf{S}^{(t)}$ improves, update $\mathbf{A}^{(t+1)} = \mathbf{S}^{(t)}$, otherwise the algorithm converges to a local optimum at $\mathbf{A}^{(t)}$. Note that the optimal step size $\eta^{(t)} \in \{0, 1\}$ remedies the non-convexity of the constraint set, as iterates are guaranteed to remain in $\mathcal{A}(T_x, T_y)$ in spite of its non-convexity.

Proposition 1. *Algorithm 1 for computing Gromov DTW converges to a stationary point.*

Proof. Appendix A. □

Algorithm 1 Franke–Wolfe algorithm for Gromov DTW

Initialize $\mathbf{A} \in \mathcal{A}(T_x, T_y)$ arbitrarily, and compute $L_{ijkl} = \mathcal{L}(d_{\mathcal{X}}(x_i, x_k), d_{\mathcal{Y}}(y_j, y_l))$.
while $\eta = 1$ **do**
 Compute $\mathbf{A} \leftarrow \arg \min_{\mathbf{A}' \in \mathcal{A}(T_x, T_y)} \langle \mathbf{L} \otimes \mathbf{A}, \mathbf{A}' \rangle_{\text{F}}$ using (2) if $\gamma = 0$ or (14) if $\gamma > 0$.
 Update η using (11)
end while
return \mathbf{A}

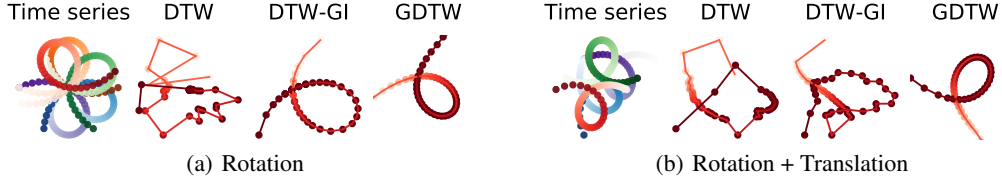


Figure 2: Barycenters of times series with DTW, DTW-GI, and GDTW. In (a) random rotations are applied to the time series, while in (b) random rotations and translations are applied.

3.2 Gromov DTW as a Loss Function

Gromov DTW can be itself used as a differentiable loss function. Here, we apply the envelope theorem [3, 17] to (9) and obtain

$$\nabla_{\mathbf{x}, \mathbf{y}} \text{GDTW}(\mathbf{x}, \mathbf{y}) = \nabla_{\mathbf{x}, \mathbf{y}} \langle \mathbf{L}(\mathbf{x}, \mathbf{y}) \otimes \mathbf{A}^*, \mathbf{A}^* \rangle_{\mathbb{F}}, \quad \mathbf{A}^* = \arg \min_{\mathcal{A}(T_x, T_y)} \mathcal{G}_{\mathbf{x}, \mathbf{y}}(\mathbf{A}). \quad (13)$$

Similarly to DTW, GDTW suffers from unpredictability when the time series is close to a change point of the optimal alignment matrix because of the discontinuity of derivatives. To remediate this, we describe how GDTW can be softened analogously to soft DTW. This allows smoother derivatives when applying it to generative modeling of time series and imitation learning. Our algorithm for computing Gromov DTW consists of successive DTW iterations. Following ideas from the Gromov-Wasserstein literature, we propose to replace the DTW operation in the iterations with a softened version, by replacing the argmin by the soft argmin in (4). A priori, it may seem that computing this is significantly more involved—however, Cuturi and Blondel [6] observed that

$$\arg \min_{\mathbf{A} \in \mathcal{A}(T_x, T_y)}^\gamma \langle \mathbf{D}, \mathbf{A} \rangle_{\mathbb{F}} = \nabla_{\mathbf{D}} \text{DTW}_\gamma(\mathbf{D}), \quad (14)$$

where $\arg \min^\gamma$ is the softened argmin in (4). Hence, (14) can be computed by reverse-mode automatic differentiation in quadratic time, and soft GDTW iterations can be performed by plugging in $\mathbf{D} = \mathbf{L} \otimes \mathbf{A}$. We approximate the derivatives by using the optimal soft alignment matrix in (13).

4 Learning with Gromov DTW as a Loss Function

We now present a range of applications of Gromov DTW, including barycentric averaging, generative modeling and imitation learning.

4.1 Barycenters

To compute barycenters of Gromov DTW (9), we extend the algorithm from Peyré et al. [20] to the sequential setting. Given time series $\mathbf{x}_1, \dots, \mathbf{x}_J \in \mathcal{X}_1^{T_1}, \dots, \mathcal{X}_J^{T_J}$ and weights $\alpha \in \Delta_J$, let $(D_{\mathbf{x}_j})_{mn} = d_{\mathcal{X}_j}(\mathbf{x}_j^{(m)}, \mathbf{x}_j^{(n)})$. For fixed $T \in \mathbb{R}$ (length of the barycentric time series), the barycenter is defined as any triple $(\mathcal{X}, d_{\mathcal{X}}, \mathbf{x})$ satisfying

$$\mathbf{D}^* = \arg \min_{\mathbf{D} \in \mathbb{R}^{T \times T}} \sum_{j=1}^J \alpha_j \text{GDTW}(\mathbf{D}, \mathbf{D}_{\mathbf{x}_j}), \quad D_{mn} = d_{\mathcal{X}}(\mathbf{x}^{(m)}, \mathbf{x}^{(n)}), \quad n, m = 1, \dots, T, \quad (15)$$

where with some abuse of notation we denote GDTW purely in terms of distance matrices. The barycentric time series can then be reconstructed by applying multi-dimensional scaling (MDS) [13] to \mathbf{D}^* , and is illustrated in Figure 2. We solve (15) by rewriting it as

$$\min_{\mathbf{D}} \min_{\mathbf{A}_1, \dots, \mathbf{A}_J \in \mathcal{A}(T_x, T_y)} \sum_{j=1}^J \alpha_j \langle \mathcal{L}(\mathbf{D}, \mathbf{D}_{\mathbf{x}_j}) \otimes \mathbf{A}_j, \mathbf{A}_j \rangle_{\mathbb{F}}, \quad (16)$$

which is solved by alternating between minimizing over $\mathbf{A}_j, j \in 1, \dots, J$ via Algorithm 1, and minimizing over \mathbf{D} for fixed \mathbf{A}_j . The latter step admits a closed-form solution given as follows.

Proposition 2. If \mathcal{L} is a square error loss, the solution to the minimization in (16) for fixed \mathbf{A}_j is

$$\mathbf{D} = \frac{\sum_{j=1}^J \alpha_j \mathbf{A}_j^T \mathbf{D}_{\mathbf{x}_j} \mathbf{A}_j}{\sum_{j=1}^J \alpha_j (\mathbf{A}_j \mathbf{1})(\mathbf{A}_j \mathbf{1})^T}, \quad (17)$$

where division \cdot/\cdot is performed element-wise, and $\mathbf{1}$ is a vector of ones.

Proof. Appendix A. □

4.2 Generative Modeling

We now use GDTW as an approach for training generative models of time series. Here, we view our dataset of time series $\mathbf{x}_1, \dots, \mathbf{x}_J \in \mathcal{X}_1^{T_1}, \dots, \mathcal{X}_J^{T_J}$ as a discrete measure $\mu = \frac{1}{J} \sum_{j=1}^J \delta_{\mathbf{x}_j}$. We define a generative model $\mu_\theta = G_{\theta\#}\nu$, where ν is a latent measure, such as an isotropic Gaussian, $G_\theta : \mathcal{Z} \rightarrow \mathcal{X}^T$ is a neural network and $G_{\theta\#}\nu$ is the pushforward measure. By nature of Gromov DTW, the generated time series do not have to live in the same space as the data. We train the model μ_θ by minimizing the entropic Wasserstein distance W_ε [5] between μ and μ_θ . For the ground cost d of W_ε , we use DTW_γ and GDTW_γ . For GDTW_γ , the objective is

$$\min_{\theta \in \Theta} W_\varepsilon(\mu, \mu_\theta) := \min_{\pi \in \Pi(\mu, \mu_\theta)} \mathbb{E}_{(\mathbf{x}, \mathbf{y}) \sim \pi} \text{GDTW}_\gamma(\mathbf{x}, \mathbf{y}) - \varepsilon H(\pi), \quad (18)$$

where H is the relative entropic regularization term. Following Genevay et al. [10], it’s also possible to use its debiased analog. $W_\varepsilon(\mu, \mu_\theta)$ is computed efficiently using the Sinkhorn algorithm [5, 23], and θ is minimized by gradient descent. This approach extends the Sinkhorn GAN of Genevay et al. [10] and the GWGAN of Bunne et al. [1] to sequential data.

4.3 Imitation Learning

We consider an imitation learning setting in which an agent needs to solve a task given the demonstration of an expert. We assume the agent has access to the true transition function \mathcal{T} over the agent’s state-space \mathcal{X} , and define a state trajectory as a time series $\mathbf{x} \in \mathcal{X}^{T_x}$. An expert state trajectory $\mathbf{y}_{exp} \in \mathcal{Y}^{T_y}$ solving a specific task, such as traversing a maze, is given. The goal is to train the agent’s parametrized policy $\pi_\theta : \mathcal{X} \rightarrow \mathcal{A}$ to solve the given task by imitating the expert’s behavior, where \mathcal{A} is the action space. To find this policy, the agent uses the model of the environment to predict state trajectories \mathbf{x}_θ under the current policy π_θ , compares these predictions with the expert’s trajectory \mathbf{y}_{exp} , and then optimizes the controller parameters θ to minimize the distance between predicted agent trajectory and observed expert trajectory. Using GDTW, our objective is

$$\min_{\theta} \text{GDTW}_\gamma(\mathbf{y}_{exp}, \mathbf{x}_\theta). \quad (19)$$

The flexibility of GDTW allows for expert trajectories defined in pixel space $\mathcal{Y} = \mathbb{R}^{32 \times 32}$, while the agent lives in $\mathcal{X} = \mathbb{R}^2$. Similarly, rollouts obtained with π_θ mimic the expert’s trajectory up to isometry. For comparison, we also consider DTW in (19), which aims to learn the same trajectory in the same space as the expert—this requires $\mathcal{X} = \mathcal{Y}$, and starting positions for the agent and expert to be identical. From a reinforcement learning perspective, the use of GDTW in (19) can be interpreted as a value estimate and gradient-based policy learning can be seen as taking value gradients [7, 11].

5 Experiments

We now assess the effectiveness of our proposals in settings in which (i) time series live in comparable spaces and where previous approaches apply, (ii) the spaces are incomparable.

Baselines: Throughout the experiments, we compare our proposal GDTW_γ to, in settings in which they apply, DTW_γ [6, 21] and its rotationally-invariant extension DTW-GI_γ for $\gamma \geq 0$ [25].

5.1 Alignment

We first evaluate GDTW on alignment tasks. We consider two settings in which \mathbf{y} is obtained by applying to \mathbf{x} (i) a rotation, and (ii) a translation followed by a rotation. DTW-GI is invariant under

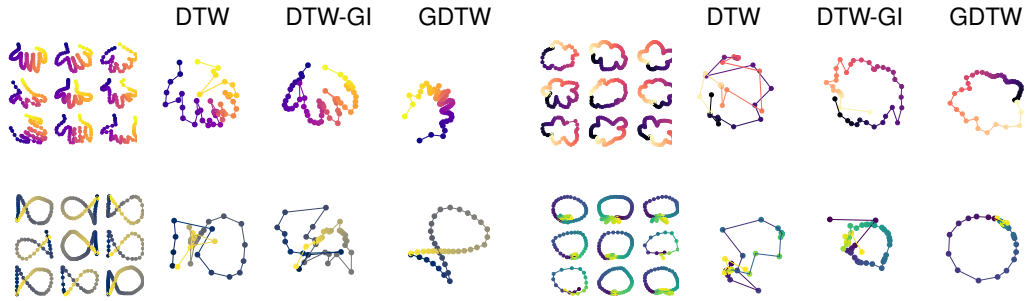


Figure 3: Barycenters computed on the QuickDraw dataset using DTW, DTW-GI and GDTW, along with sample data points from each of the four different classes (*hands*, *clouds*, *fishes*, *blueberries*).

rotations, and is therefore expected to work in setting (i) only, whilst GDTW is invariant under isometries, and is expected to work in both. In Figure 1, we see that GDTW recovers the right alignment in both settings, while DTW-GI only works in the rotational setting 1(a), and ordinary DTW fails in 1(a)–1(b). Further experiments with soft DTW and GDTW are given in Appendix B.

5.2 Barycenter Computation

We now investigate barycentric averaging of GDTW, on both toy data and the QuickDraw² dataset. We compare Gromov DTW to DTW and DTW-GI, where barycenters from the latter two methods are computed using DTW barycentric averaging [18].

Toy data In Figure 2, we see that in comparable settings DTW barycenters fail if time series are rotated or translated. DTW-GI is robust to rotation, but fails when applying both rotations and translations. By contrast, GDTW is robust to both, and leads to meaningful barycenters in all settings.

QuickDraw dataset The QuickDraw dataset consists of time series of drawings in \mathbb{R}^2 , belonging to 345 categories. Among those categories, we selected *hands*, *clouds*, *fishes*, and *blueberries*. To address high variability in classes, we selected input data following a preprocessing routine described in Appendix B. A sample of the data sets, together with barycenters computed with DTW, DTW-GI, and GDTW is displayed in Figure 3. While DTW and DTW-GI fail to reproduce the shape of the inputs for most classes, GDTW provides meaningful barycenters across the range of examples. This shows that GDTW is more robust in recovering the geometric shape of the time series, whilst DTW variants are sensitive to moderate isometries.

5.3 Generative Modeling

We evaluate the generative modeling proposal of Section 4.2, and compare the behavior of the learned model when using DTW and GDTW. Here, we consider the sequential-MNIST dataset³, which consists of time series of digits in \mathbb{R}^2 being drawn, and where each time step corresponds to a stroke. In Figure 4 we see that samples using GDTW as ground cost (18) are of a significantly better quality



Figure 4: Samples generated by the time series GAN trained on Sequential MNIST, with DTW_γ and GDTW_γ , respectively, used as ground costs.

²[HTTPS://QUICKDRAW.WITHGOOGLE.COM/](https://quickdraw.withgoogle.com/)

³[HTTPS://GITHUB.COM/EDWIN-DE-JONG/MNIST-DIGITS-STROKE-SEQUENCE-DATA](https://github.com/edwin-de-jong/mnist-digits-stroke-sequence-data)

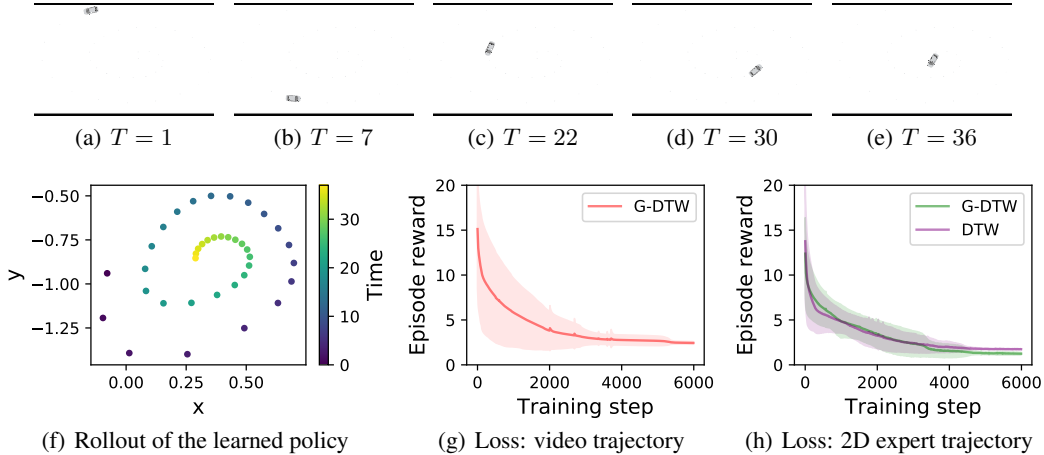


Figure 5: (a)–(e): Expert trajectory (sequence of pixel images); (f): policy of an agent in \mathbb{R}^2 learned by imitation learning given video demonstrations; (g): log-episodic loss per training step in the video/2D setting; (h) in the 2D/2D setting (averaged across 20 seeds, with standard deviations).

than samples using DTW. This can be explained by the variability in the data set: slight translations significantly affect DTW, but not GDTW. Note that the GDTW samples are rotated and reflected, since GDTW only produces learned samples up to metric isometries.

5.4 Imitation Learning

We now apply Gromov DTW to the imitation learning setting of Section 4.3. Here, we are given an expert trajectory \mathbf{y}_{exp} , and our goal is to find a policy π_{θ} such that the agent’s simulated trajectory \mathbf{x}_{θ} mimics \mathbf{y}_{exp} . We consider maze navigation tasks in two settings: (i) both expert trajectories and the agent’s domain are $\mathcal{X} = \mathcal{Y} = \mathbb{R}^2$ and (ii) expert trajectories consist of a video sequence of 32×32 images, giving $\mathcal{Y} = \mathbb{R}^{32 \times 32}$, whilst the agent’s domain is $\mathcal{X} = \mathbb{R}^2$. In the first setting, DTW and GDTW apply, whilst in the second setting only GDTW can be used. Figure 5(h) displays the loss (19), which is the GDTW distance to the given trajectory, obtained by learning with GDTW and DTW in (i) averaged across 20 seeds. We see that GDTW slightly outperforms DTW, and both agents recover the spiral trajectory provided by the expert.

Finally, we consider a setting in which an agent living in \mathbb{R}^2 is provided with an expert trajectory \mathbf{y}_{exp} consisting of a video of a car driving through a spiral, illustrated in Figures 5(a)–5(e) (before down-scaling the images). Here, the state-space of the agent, $\mathcal{X} = \mathbb{R}^2$, differs from the state-space of the expert, $\mathcal{Y} = \mathbb{R}^{32 \times 32}$. We define the cost on image space $d_{\mathcal{Y}}$ to be the 2-Wasserstein distance, defined on images interpreted as densities on a grid, and the cost on the Euclidean space $d_{\mathcal{X}}$ to be the Euclidean distance. Figure 5(f) shows the agent’s trajectory under the learned policy π_{θ} , and Figure 5(g) shows the loss (19) against the number of training steps. We see that, using GDTW, the agent successfully learns to solve the task despite never having access to trajectories in the space of interest.

6 Conclusion

We propose Gromov DTW, a distance between time-series living on potentially incomparable spaces. The idea is to consider the intra-relational geometries of the considered time series, alleviating the need for a ground metric to be defined across spaces, which is a requirement of previous approaches. Moreover, Gromov DTW is invariant under isometries by nature, which is an important inductive bias for generalization, and makes it significantly more robust under transformations of the spaces by contrast with DTW and DTW-GI. The generality of our proposed distance enables applying it to a wide range of problems that previous approaches could not tackle, in particular when comparing time series on unregistered spaces. We considered applications ranging from alignment to barycentric averaging, generative modeling and imitation learning.

Broader Impact

In this work, we develop techniques for aligning, averaging, and learning using multiple time series in potentially different domains. This makes it easier for practitioners to use a number of different tools in these settings.

In particular, we envision this might help reduce demand for manually labeled data in robotics. For example, one might use techniques derived from ours to train robots on expert demonstrations, without manually transcribing those demonstrations into a computer-friendly format. This can play an important role in human-robot interaction, for instance in construction or elderly care.

Similarly, aligning time series can be helpful in epidemiology. For example, it could allow scientists to compare the shapes of infection curves with different starting points, thereby allowing to compare countries at different stages of an epidemic. This could help with understanding the evolution of diseases, such as COVID-19, which would in turn benefit the general public.

Finally, our work can be used in a climate science context to align time series from computer-generated numerical weather prediction and heterogeneous observational data, which might be available with different sampling frequencies. This in turn might improve quality of data assimilation, thereby improving weather forecasting, which we hope might contribute to the United Nations’ sustainable development goal 13 on climate action.

Acknowledgements

We are grateful to K. S. Sesh Kumar for ideas on the Frank-Wolfe algorithm. SC was supported by the Engineering and Physical Sciences Research Council (grant number EP/S021566/1).

References

- [1] C. Bunne, D. Alvarez-Melis, A. Krause, and S. Jegelka. Learning Generative Models Across Incomparable Spaces. In *ICML*, 2019. Cited on pages [3](#), [6](#).
- [2] Byoung-Kee Yi, H. V. Jagadish, and C. Faloutsos. Efficient Retrieval of Similar Time Sequences Under Time Warping. In *ICDE*, 1998. Cited on page [2](#).
- [3] M. Carter. *Foundations of Mathematical Economics*. MIT Press. 2001. Cited on page [5](#).
- [4] L. Chapel, M. Z. Alaya, and G. Gasso. Partial Gromov-Wasserstein with Applications on Positive-Unlabeled Learning. *arXiv:2002.08276*, 2020. Cited on pages [4](#), [13](#).
- [5] M. Cuturi. Sinkhorn Distances: Lightspeed Computation of Optimal Transport. In *NeurIPS*. 2013. Cited on page [6](#).
- [6] M. Cuturi and M. Blondel. Soft-DTW: A Differentiable Loss Function for Time-Series. In *ICML*, 2017. Cited on pages [1](#), [2](#), [5](#), [6](#).
- [7] M. Fairbank and E. Alonso. Value-Gradient Learning. In *IJCNN*, 2012. Cited on page [6](#).
- [8] J. Feydy, T. Séjourné, F.-X. Vialard, S.-i. Amari, A. Trounev, and G. Peyré. Interpolating Between Optimal Transport and MMD Using Sinkhorn Divergences. In *AISTATS*, 2019. Cited on page [14](#).
- [9] M. Frank and P. Wolfe. An Algorithm for Quadratic Programming. *Naval Research Logistics Quarterly*, 3(1–2):95–110, 1956. Cited on pages [4](#), [12](#).
- [10] A. Genevay, G. Peyre, and M. Cuturi. Learning Generative Models with Sinkhorn Divergences. In *AISTATS*, 2018. Cited on page [6](#).
- [11] N. Heess, G. Wayne, D. Silver, T. Lillicrap, T. Erez, and Y. Tassa. Learning Continuous Control Policies by Stochastic Value Gradients. In *NeurIPS*, 2015. Cited on page [6](#).
- [12] R. J. Kate. Using Dynamic Time Warping Distances as Features for Improved Time Series Classification. *Data Mining Knowledge Discovery*, 30(2):283–312, 2016. Cited on page [2](#).
- [13] J. B. Kruskal and M. Wish. *Multidimensional Scaling*. Sage Publications, 1978. Cited on page [5](#).
- [14] S. Lacoste-Julien. Convergence Rate of Frank-Wolfe for Non-Convex Objectives. *arXiv:1607.00345*, 2016. Cited on page [13](#).
- [15] D. Lemire. Faster Retrieval with a Two-Pass Dynamic-Time-Warping Lower Bound. *Pattern Recognition*, 42:2169–2180, 2009. Cited on pages [11](#), [12](#).

- [16] F. Mémoli. Gromov-Wasserstein Distances and the Metric Approach to Object Matching. *Foundations of Computational Mathematics*, 11(4):417–487, 2011. Cited on pages [2](#), [3](#).
- [17] P. Milgrom and I. Segal. Envelope Theorems for Arbitrary Choice Sets. *Econometrica*, 70:583–601, 2002. Cited on page [5](#).
- [18] F. Petitjean and P. Gañçarski. Summarizing a Set of Time Series by Averaging: From Steiner Sequence to Compact Multiple Alignment. *Theoretical Computer Science*, 414:76–91, 2012. Cited on pages [2](#), [7](#).
- [19] G. Peyré and M. Cuturi. Computational Optimal Transport. *Foundations and Trends in Machine Learning*, 11(5–6):355–607, 2019. Cited on page [3](#).
- [20] G. Peyré, M. Cuturi, and J. Solomon. Gromov-Wasserstein Averaging of Kernel and Distance Matrices. In *ICML*, 2016. Cited on pages [4](#), [5](#).
- [21] H. Sakoe and S. Chiba. Dynamic Programming Algorithm Optimization for Spoken Word Recognition. *ICASSP*, 1978. Cited on pages [1](#), [2](#), [6](#).
- [22] D. Schultz and B. Jain. Nonsmooth Analysis and Subgradient Methods for Averaging in Dynamic Time Warping Spaces. *Pattern Recognition*, 74:340–358, 2018. Cited on page [2](#).
- [23] R. Sinkhorn. Diagonal Equivalence to Matrices with Prescribed Row and Column Sums. In 1974. Cited on page [6](#).
- [24] J. Solomon, G. Peyre, V. G. Kim, and S. Sra. Entropic Metric Alignment for Correspondence Problems. *SIGGRAPH*, 2016. Cited on page [3](#).
- [25] T. Vayer, L. Chapel, N. Courty, R. Flamary, Y. Soullard, and R. Tavenard. Time Series Alignment with Global Invariances. *arXiv:2002.03848*, 2020. Cited on pages [1–3](#), [6](#).
- [26] T. Vayer, N. Courty, R. Tavenard, C. Laetitia, and R. Flamary. Optimal Transport for Structured Data with Application on Graphs. In *ICML*, 2019. Cited on page [3](#).
- [27] C. Villani. *Optimal Transport: Old and New*, volume 338. Springer Science & Business Media, 2008. Cited on pages [3](#), [11](#).
- [28] H. Xu, D. Luo, and L. Carin. Scalable Gromov-Wasserstein Learning for Graph Partitioning and Matching. In *NeurIPS*. 2019. Cited on page [3](#).
- [29] H. Xu, D. Luo, H. Zha, and L. C. Duke. Gromov-Wasserstein Learning for Graph Matching and Node Embedding. In *ICML*, 2019. Cited on page [3](#).

A Theory

Metric Properties

Here we develop the theory of Gromov dynamic time warping distances. We begin by introducing the necessary preliminaries.

Definition 3 (Time series). *Let $(\mathcal{X}, d_{\mathcal{X}})$ be a compact metric space, and let $I_{\mathcal{X}} = \{1, 2, \dots, T_{\mathcal{X}}\} \subset \mathbb{N}$. We call a finite sequence $\mathbf{x} : I_{\mathcal{X}} \rightarrow \mathcal{X}$ a TIME SERIES. Let X be the space of all time series.*

Definition 4. *Let \mathbf{x} and \mathbf{y} be time series. Define a premetric $D : \mathcal{X} \times \mathcal{Y} \rightarrow \mathbb{R}$, which we call the COST. Define the $m \times n$ COST MATRIX $\mathbf{D} \in \mathbb{R}^{m \times n}$ by $D_{ij} = D(x_i, y_j)$.*

Definition 5. *We say that a binary matrix \mathbf{A} is an ALIGNMENT MATRIX if $A_{11} = 1$, $A_{mn} = 1$, and $A_{ij} = 1$ implies exactly one of $A_{i-1,j} = 1$, $A_{i,j-1} = 1$, and $A_{i-1,j-1} = 1$ holds. Let*

$$\mathcal{A} = \{\mathbf{A} \in \{0, 1\}^{m \times n} : \mathbf{A} \text{ is an alignment matrix}\} \quad (20)$$

be the set of ALIGNMENT MATRICES.

Definition 6 (Dynamic Time Warping). *Let \mathbf{x} and \mathbf{y} be time series. Define the DYNAMIC TIME WARPING distance by*

$$\text{DTW}(\mathbf{x}, \mathbf{y}) = \min_{\mathbf{A} \in \mathcal{A}} \langle \mathbf{D}, \mathbf{A} \rangle_{\text{F}}, \quad (21)$$

where $\langle \cdot, \cdot \rangle_{\text{F}}$ is the Frobenius norm over real matrices.

Proposition 7. *If D is a premetric, then $\text{DTW} : X \times X \rightarrow \mathbb{R}$ is a premetric on the space of time series. If we take $c = d_M$, then $\text{DTW} : X \times X \rightarrow \mathbb{R}$ is a symmetric premetric on X .*

Proof. Lemire [15]. □

A premetric induces a Hausdorff topology on the set it is defined over, and so is suitable for many purposes that ordinary metrics are used for. To proceed along the path suggested by Gromov-Hausdorff and Gromov-Wasserstein distances over metric-measure spaces, we need to define the time series analog.

Definition 8. *Define a METRIC SPACE EQUIPPED WITH A TIME SERIES to be a triple $(\mathcal{X}, d_{\mathcal{X}}, \mathbf{x})$.*

Definition 9. *Let $(\mathcal{X}, d_{\mathcal{X}}, \mathbf{x})$ and $(\mathcal{Y}, d_{\mathcal{Y}}, \mathbf{y})$ be metric spaces equipped with time series. Define $X|_{\mathbf{x}} = \{x \in X : x \in \text{img } \mathbf{x}\}$, and $Y|_{\mathbf{y}}$ similarly, and equip both sets with their respective subset metrics. We say that $(\mathcal{X}, d_{\mathcal{X}}, \mathbf{x})$ and $(\mathcal{Y}, d_{\mathcal{Y}}, \mathbf{y})$ are ISOMORPHIC if there is a metric isometry $\phi : X|_{\mathbf{x}} \rightarrow Y|_{\mathbf{y}}$ such that $\phi(\hat{x}_i) = \hat{y}_i$, where \hat{x} and \hat{y} denote \mathbf{x} and \mathbf{y} with consecutive repeated elements removed.*

At this stage it is not clear whether or not the class of all such triples under isometry forms a set, or is instead a proper class. To avoid set-theoretic complications, we need the following technical result.

Result 10. *The class of all isometry classes of compact metric spaces is a set.*

Proof. Villani [27, ch. 27, p. 746]. □

It follows immediately that the class of all metric spaces equipped with time series is a set, provided that identification by isometry extends to the time series. We are now ready to define GDTW.

Definition 11. *Let \mathcal{L} be a premetric on \mathbb{R}^+ , and define $\mathcal{L} \in \mathbb{R}^{m \times n \times m \times n}$ by*

$$\mathcal{L}_{ijkl} = \mathcal{L}(d_{\mathcal{X}}(x_i, x_k), d_{\mathcal{Y}}(y_j, y_l)). \quad (22)$$

Define the GROMOV DYNAMIC TIME WARPING distance by

$$\text{GDTW}((\mathcal{X}, d_{\mathcal{X}}, \mathbf{x}), (\mathcal{Y}, d_{\mathcal{Y}}, \mathbf{y})) = \min_{\mathbf{A} \in \mathcal{A}} \langle \mathcal{L} \otimes \mathbf{A}, \mathbf{A} \rangle_{\text{F}}, \quad (23)$$

where $(\mathcal{L} \otimes \mathbf{A})_{ij} = \sum_{kl} \mathcal{L}_{ijkl} A_{kl}$.

Proposition 12. *GDTW is a premetric on the set of all metric spaces equipped with time series.*

Proof. We check the conditions. Non-negativity is immediate by definition. It also follows immediately that $(\mathcal{X}, d_{\mathcal{X}}, \mathbf{x}) \cong (\mathcal{Y}, d_{\mathcal{Y}}, \mathbf{y})$ implies $\text{GDTW}((\mathcal{X}, d_{\mathcal{X}}, \mathbf{x}), (\mathcal{Y}, d_{\mathcal{Y}}, \mathbf{y})) = 0$. We thus need to prove that $\text{GDTW}((\mathcal{X}, d_{\mathcal{X}}, \mathbf{x}), (\mathcal{Y}, d_{\mathcal{Y}}, \mathbf{y})) = 0$ implies $(\mathcal{X}, d_{\mathcal{X}}, \mathbf{x}) \cong (\mathcal{Y}, d_{\mathcal{Y}}, \mathbf{y})$. By hypothesis, we have

$$\text{GDTW}((\mathcal{X}, d_{\mathcal{X}}, \mathbf{x}), (\mathcal{Y}, d_{\mathcal{Y}}, \mathbf{y})) = \sum_{ijkl} A_{ij} \mathcal{L}_{ijkl} A_{kl} = \sum_{\substack{A_{ij}=1 \\ A_{kl}=1}} \mathcal{L}_{ijkl}, \quad (24)$$

where all elements of the last sum are non-zero. Suppose without loss of generality that \mathbf{x} and \mathbf{y} contain no duplicate elements. We argue inductively that optimal \mathbf{A} is the identity matrix.

1. First, note that $A_{11} = 1$ by definition of \mathbf{A} .
2. Now, consider A_{21} . If we suppose $A_{21} = 1$, then we must have $\mathcal{L}_{2111} = 0$, and hence $d_{\mathcal{X}}(x_2, x_1) = d_{\mathcal{Y}}(y_1, y_1) = 0$. But then $x_2 = x_1$, contradicting the assumption there are no duplicates. Hence, $A_{21} = 0$.
3. By mirroring the above argument, $A_{12} = 0$. Hence, by definition of \mathbf{A} , the only remaining possibility is $A_{22} = 1$. Inductively, we conclude $A_{ii} = 1$ for all i , and $A_{ij} = 0$ for $i \neq j$.
4. Finally, since the lower-right corner of \mathbf{A} has to also be equal to one by definition, it follows that \mathbf{A} is the square identity matrix.

Hence $A_{ij} = 1$ and $A_{kl} = 1$ if and only if $i = j$ and $k = l$. Plugging this into the previous equality yields $d_{\mathcal{X}}(x_i, x_k) = d_{\mathcal{Y}}(y_i, y_k)$ for all i, k , which together with diagonal \mathbf{A} gives the isomorphism. Finally, to see that lack of duplicates truly is assumed without loss of generality, note that if there are duplicates in \mathbf{x} and \mathbf{y} , then we apply the above argument to $\hat{\mathbf{x}}$ and $\hat{\mathbf{y}}$ of Definition 9, which no longer contain duplicates. The claim follows. \square

One can easily see that GDTW will be symmetric if L is symmetric. Since DTW itself doesn't satisfy a triangle inequality [15], GDTW won't satisfy it either.

Frank–Wolfe Algorithm

We formulate an algorithm for computing GDTW within the Frank–Wolfe (FW) framework [9]. These algorithms tackle problems of the form

$$\min_{\mathbf{A} \in \mathcal{C}} \mathcal{G}(\mathbf{A}), \quad (25)$$

where $\mathcal{G} : \mathbb{R}^d \rightarrow \mathbb{R}$ is the objective to be minimized, assumed differentiable with Lipschitz continuous gradient, and $\mathcal{C} \subseteq \mathbb{R}^d$ is the (usually convex) constraint set.

We first describe the Frank–Wolfe algorithm in its general form. Let be $\mathbf{A}^{(0)}$ the initial point.

1. Solve the linear minimization oracle

$$\mathbf{S}^{(t)} = \arg \min_{\mathbf{A} \in \mathcal{C}} \langle \nabla_{\mathbf{A}} \mathcal{G}(\mathbf{A}^{(t)}), \mathbf{A} \rangle. \quad (26)$$

2. Find the optimal step size

$$\gamma^{(t)} = \arg \min_{\gamma \in [0,1]} \mathcal{G}(\mathbf{A}^{(t)} + \gamma(\mathbf{S}^{(t)} - \mathbf{A}^{(t)})). \quad (27)$$

3. Perform the update

$$\mathbf{A}^{(t+1)} = \mathbf{A}^{(t)} + \gamma^{(t)}(\mathbf{S}^{(t)} - \mathbf{A}^{(t)}). \quad (28)$$

We now describe the algorithm our setting. The objective is

$$\min_{\mathbf{A} \in \mathcal{A}(T_x, T_y)} \mathcal{G}(\mathbf{A}), \quad \mathcal{G}(\mathbf{A}) = \langle \mathbf{L} \otimes \mathbf{A}, \mathbf{A} \rangle = \sum_{ijkl} L_{ijkl} A_{ij} A_{kl}. \quad (29)$$

The constraint domain $\mathcal{A}(T_x, T_y)$ in our case is not convex. This is usually a requirement of Frank–Wolfe algorithms, but we derive a result in the sequel that enables us to bypass this requirement.

Step 1: Linear Minimization Oracle We note that the gradient is of the form

$$\nabla \mathcal{G}(\mathbf{A}) = \mathbf{L} \otimes \mathbf{A} \quad (30)$$

and step 1 thus consists in solving

$$\arg \min_{\mathbf{A} \in \mathcal{A}(T_x, T_y)} \left\langle \mathbf{L} \otimes \mathbf{A}^{(t)}, \mathbf{A} \right\rangle. \quad (31)$$

This can be minimized exactly in $O(T_x T_y)$ time by plugging $\mathbf{D} = \mathbf{L} \otimes \mathbf{A}^{(t)}$ in the DTW objective (1) and solving via dynamic programming.

Step 2: Optimal Step Size

Proposition 13. *The optimal step size in (27) is either 0 or 1.*

Proof. This follows by applying the argument of Chapel et al. [4], who derive a similar result in the Gromov–Wasserstein setting, with one minor modification. In their equation (9), an optimal-transport-based argument is used to obtain an inequality—in our setting, an analogous inequality holds for DTW, given by

$$\left\langle \mathbf{L} \otimes \mathbf{A}^{(t)}, \mathbf{S}^{(t)} \right\rangle \leq \left\langle \mathbf{L} \otimes \mathbf{A}^{(t)}, \mathbf{A}^{(t)} \right\rangle, \quad (32)$$

where \mathbf{S}_t is given by dynamic programming. The claim follows. \square

We observe from Proposition 13 that the optimal step size is 0 or 1, therefore if the proposal $\mathbf{S}^{(t)}$ improves on the objective, $\gamma^{(t)} = 1$, otherwise $\gamma^{(t)} = 0$.

Step 3: Iterative Updates We set

$$\mathbf{x}^{(t+1)} = \begin{cases} \mathbf{S}^{(t)} & \text{if } \gamma^{(t)} = 1 \\ \mathbf{A}^{(t)} & \text{if } \gamma^{(t)} = 0. \end{cases} \quad (33)$$

Frank–Wolfe algorithms typically require convexity of the constraint set \mathcal{C} , otherwise the iterates $\mathbf{A}^{(t+1)} = \mathbf{A}^{(t)} + \gamma^{(t)}(\mathbf{S}^{(t)} - \mathbf{A}^{(t)})$ might escape from the constrained domain. In our setting, since the optimal step size is either 0 or 1, this never happens: $\mathbf{A}^{(t+1)}$ is equal to $\mathbf{A}^{(t)}$ or $\mathbf{S}^{(t)}$, and both belong to the constraint set, and convexity is not needed to guarantee the iterates remain in the constrained domain.

Summarizing, we obtain the following.

Proposition 14. *Algorithm 1 for computing GDTW converges to a stationary point.*

Proof. The result follows by a minor modification of Theorem 1 of Lacoste-Julien [14], which proves convergence of the Frank–Wolfe algorithm for possibly non-convex optimization objectives over convex constraint sets. Here, we use Proposition 13 instead of convexity to ensure the iterates remain in the constraint set. \square

Barycenter computation

Proposition 15. *If \mathcal{L} is a square error loss, the solution to the minimization in (16) for fixed \mathbf{A}_j is*

$$\mathbf{D} = \sum_{j=1}^J \alpha_j \mathbf{A}_j^T \mathbf{D}_{\mathbf{x}_j} \mathbf{A}_j / \sum_{j=1}^J \alpha_j (\mathbf{A}_j \mathbf{1})(\mathbf{A}_j \mathbf{1})^T, \quad (34)$$

where division \cdot / \cdot is performed element-wise, and $\mathbf{1}$ is a vector of ones.

Proof. If \mathcal{L} is square error loss, then (16) can be written as

$$\min_{\mathbf{D}} \sum_{j=1}^J \alpha_j \left\langle \mathbf{D} \odot \mathbf{D} \mathbf{A}_j \mathbf{1} \mathbf{1}^T + \mathbf{1} \mathbf{1}^T \mathbf{A}_j \mathbf{D}_{\mathbf{x}_j} \odot \mathbf{D}_{\mathbf{x}_j} - 2 \mathbf{D} \mathbf{A}_j \mathbf{D}_{\mathbf{x}_j}^T, \mathbf{A}_j \right\rangle_{\mathbb{F}}, \quad (35)$$

where \odot is element-wise matrix multiplication. Differentiating the objective with respect to \mathbf{D} and setting it equal to 0, we get

$$\mathbf{D} \odot \left(\sum_{j=1}^J \alpha_j (\mathbf{A}_j \mathbf{1})(\mathbf{1}^T \mathbf{A}_j^T) \right) = \sum_j \alpha_j \mathbf{A}_j^T \mathbf{D} \mathbf{x}_j \mathbf{A}_j, \quad (36)$$

which, dividing both sides element-wise, gives the result. \square

B Experimental Details

Alignments

In Figures 7–10, we provide further alignment experiments. Here, we set the entropic term γ to 1 for soft alignments, and we use normalized distance matrices. We observe that GDTW and soft GDTW are robust to scaling, rotations and translations, whilst DTW and soft DTW are sensitive to rotations and translations. Finally, DTW-GI is robust to rotations, but sensitive to translations, which further corroborates the observations from Figure 1.

Barycenters

In this experiment, we perform barycenters of 30 elements of 4 quickdraw classes with respect to DTW, DTW-GI and GDTW.

Data selection and pre-processing The classes considered in the experiment are *fish*, *blueberries*, *clouds* and *hands*. The variability in each class of QuickDraw is extremely high: we created datasets of 30 elements such that it is straightforward to recognize to which category the element belongs to, such that the element is drawn with a single stroke and such that it has a common style. The full datasets are displayed in Figure 6. Before running the algorithms, we rescaled the data, applying the transformation $\mathbf{x} \mapsto (\mathbf{x} - \min(\mathbf{x})) / \max(\mathbf{x})$ to each data point. Finally, we down-sampled the length of the time series reducing it by 1/3 for *hands* and 1/2 for *fish*, *clouds* and *blueberries*.

Algorithms For GDTW barycenters, we applied our algorithm of Section 4.1, using the entropy regularized version of GDTW with $\gamma = 1$. For DTW and DTW-GI, we used standard DBA procedures. For both algorithms, we set the barycentric length to 60 for *fish* and *hands* and 40 for *clouds* and *blueberries*. Also, we set the maximum number of FW iterations for GDTW to 25, and the number of DTW-GI iterations to 30.

Generative Modeling

In this experiment, we use the Sinkhorn divergence objective. We use a latent dimension of 15, and the generator is a 4-layer MLP with 1000 neurons per layers. The length of the generated time series is set to $T = 40$, and the dimension of the space is $p = 2$, thus the MLP’s output dimension is $T \times p = 80$. We set the batch size to 25. We use the ADAM optimizer, with $\beta = (0.5, 0.99)$, and the learning rate set to 5×10^{-5} . We set $\gamma = 1$, and the maximum number of iterations in the GDTW computation to 10. We use the sequential MNIST dataset⁴ and normalize the data, which time series in \mathbb{R}^2 , into the unit square.

Imitation Learning

In this experiment, we use a two-layer MLP policy, with input dimension of $\dim(\mathcal{X})$, a hidden dimension of 64, and an output dimension of 2. The learning rate is set to 5×10^{-5} , and we use the ADAM optimizer, and $\beta = (0.5, 0.99)$. In the video/2D experiment⁵, the ground cost for the video is entropic 2-Wasserstein distance, computed efficiently using GEOMLOSS [8], and the ground cost on the 2D space is squared error loss. We plot mean scores along with standard deviations (across 20 random seeds).

⁴Sequential MNIST: [HTTPS://GITHUB.COM/EDWIN-DE-JONG/MNIST-DIGITS-STROKE-SEQUENCE-DATA](https://github.com/edwin-de-jong/mnist-digits-stroke-sequence-data).

⁵The video was generated using [HTTPS://GITHUB.COM/GEZICHTSHAAR/PYRACEGAME](https://github.com/gezichtshaar/pyracegame).

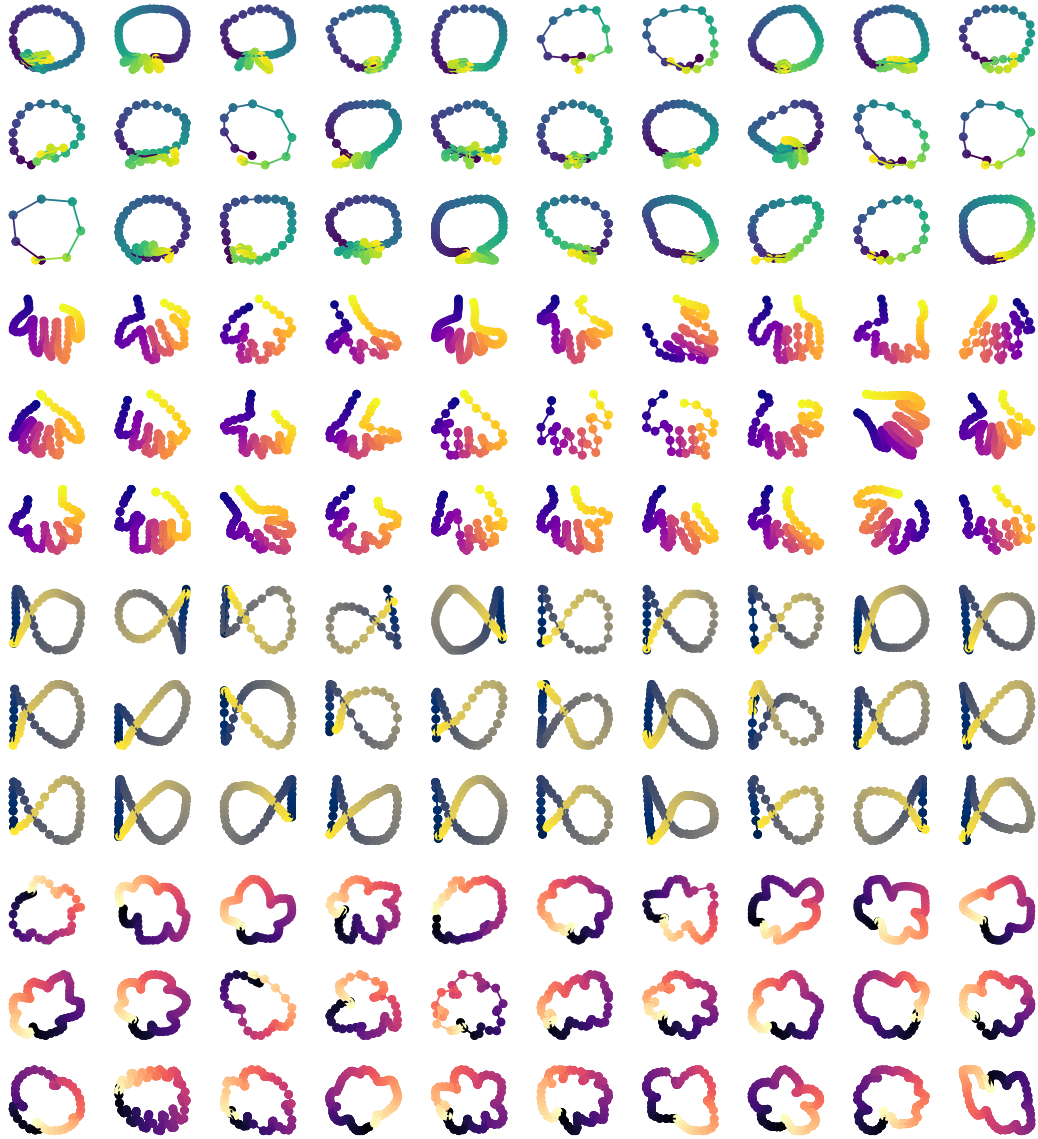


Figure 6: Quickdraw datasets, with classes *blueberries*, *hands*, *fishes*, *clouds*.

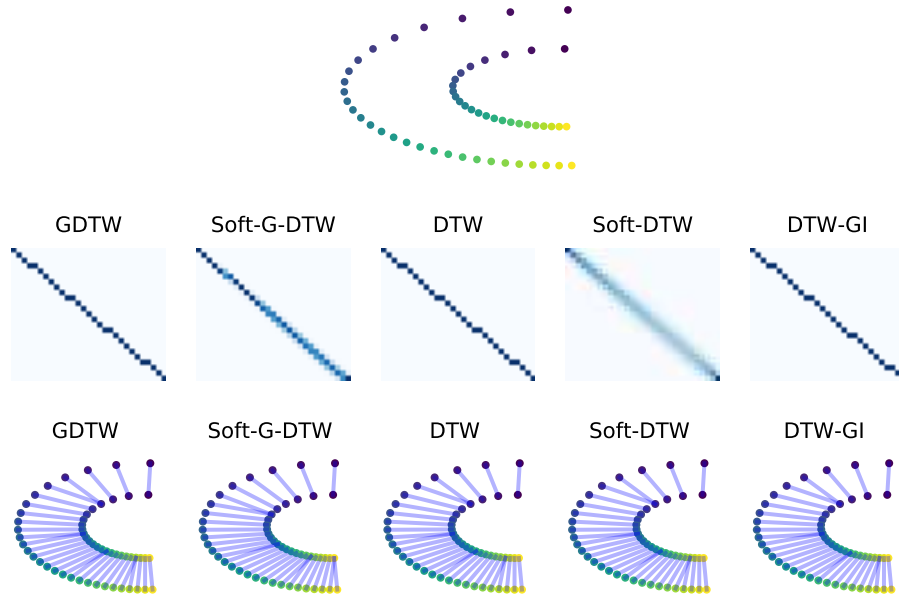


Figure 7: Two time series (top) along with alignment matrices (middle) and alignments with different approaches. In this example, all methods provide a sensible alignment because the time series are on the same axis of rotation and close in the ground space.

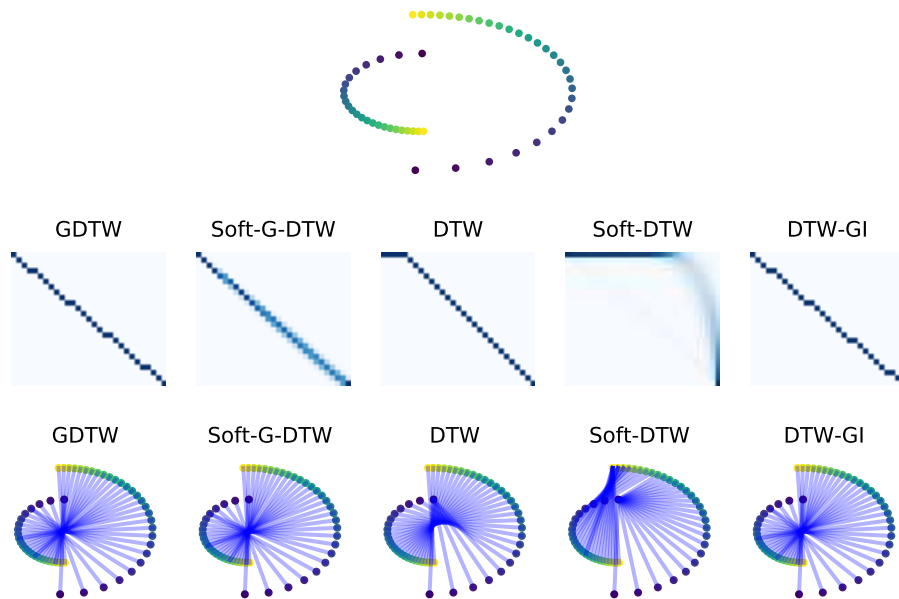


Figure 8: Two time series (top), alignment matrices (middle) and alignments with different approaches. In this example, the time series are not on the same rotation axis which makes DTW variants fail, whilst GDTW and DTW-GI provide good alignments due to rotational invariance.

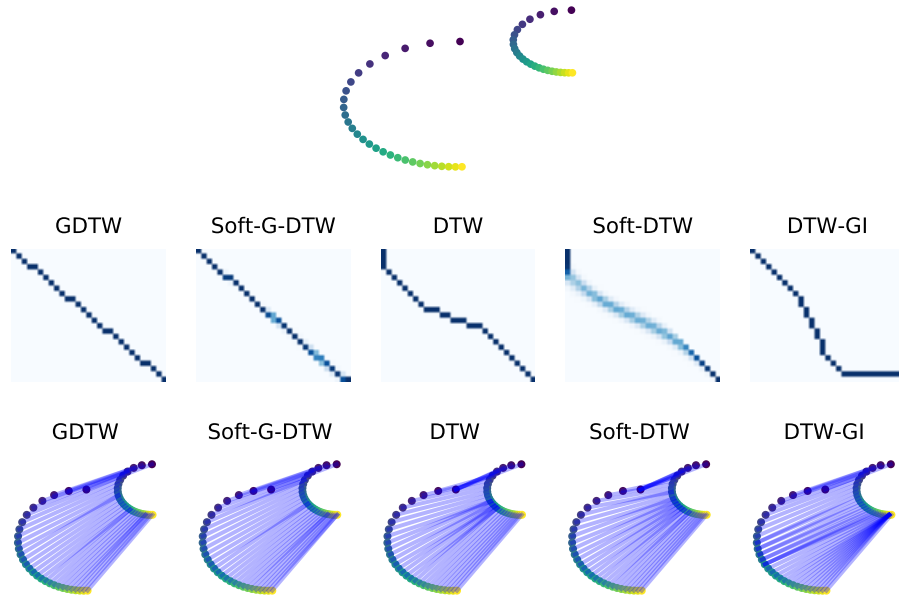


Figure 9: Two time series (top) along with alignment matrices (middle) and alignments with different approaches. In this example, the time series are translated which makes DTW variants and DTW-GI fail, whilst GDTW is invariant to all isometries, and is thus robust to such transformation.

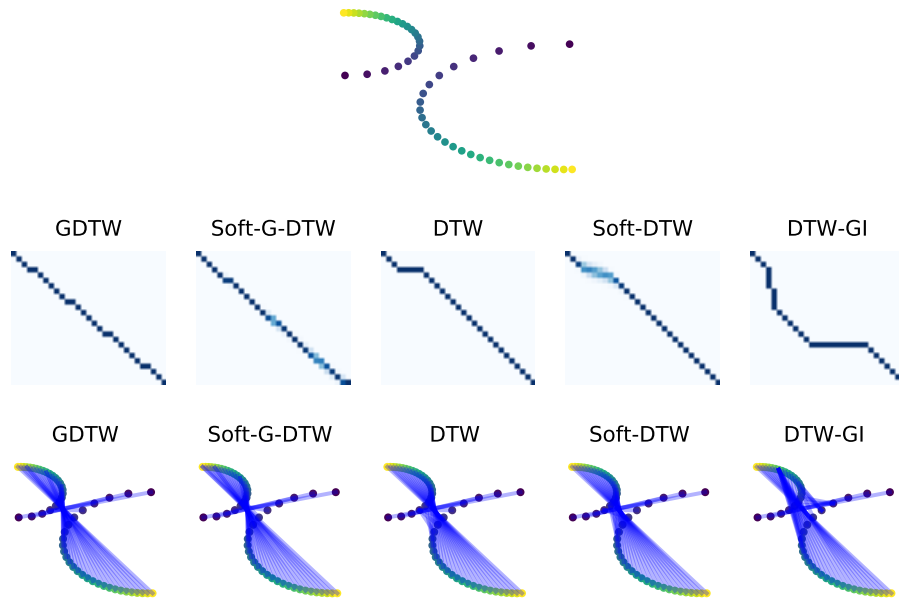


Figure 10: Two time series (top) along with alignment matrices (middle) and alignments with different approaches. In this example, the time series are rotated and translated which makes DTW variants and DTW-GI fail, whilst GDTW is invariant to all isometries, and is thus robust to such transformations.